

Periodic orbit quantization of a weakly interacting two-body system using perturbed symmetry-broken trace formulas

Jamal Sakhr,^{1,*} Randall S. Dumont,² and Niall D. Whelan¹

¹*Department of Physics and Astronomy, McMaster University, Hamilton, Ontario, Canada L8S 4M1*

²*Department of Chemistry, McMaster University, Hamilton, Ontario, Canada L8S 4M1*

(Received 13 August 2006; published 3 November 2006)

The semiclassical limit of the quantum few-body problem has not been studied in general terms from the point of view of periodic orbit theory. In a previous paper, we studied noninteracting two-body systems [Phys. Rev. A **62**, 042109 (2000)] and discussed the fact that the periodic orbits occur in continuous families. Interactions destroy the periodic orbit families leaving a discrete set of isolated periodic orbits. In this paper, we consider the effect of weak two-body interactions, which can be thought of as symmetry-breaking perturbations and can thus be analyzed using a theory developed by Creagh [Ann. Phys. (N.Y.) **248**, 1 (1996)]. The Pöschl-Teller two-body system confined in a square well is analyzed to illustrate the use of the formalism. It is shown that the effect of the interaction can be evaluated for all two-particle periodic orbits, and that the coarse-grained quantum density of states can be fully reproduced from simply summing the perturbed contributions of each periodic orbit family. Good numerical estimates of the quantum singlet energies can actually be obtained, but it is found that that perturbed trace formulas cannot reproduce the multiplet splittings predicted from quantum mechanics. Several interesting properties are observed depending on the range of the interaction and on whether the interaction is attractive or repulsive.

DOI: [10.1103/PhysRevA.74.052104](https://doi.org/10.1103/PhysRevA.74.052104)

PACS number(s): 03.65.Sq, 05.45.Mt, 45.50.Jf

I. INTRODUCTION

Semiclassical theory emerged at the advent of quantum mechanics and has evolved into a powerful tool for performing analytical calculations and for gaining insight into new problems [1]. The most important energy domain semiclassical theory is periodic orbit theory (POT), which extracts spectral information from knowledge of the classical periodic orbits. For nonintegrable systems, the central result of periodic orbit theory is the Gutzwiller trace formula [1–5], which expresses the oscillatory part of the density of states as an infinite sum over the periodic orbits of the classical system. Although conceptually elegant, the Gutzwiller trace formula is generally very hard to use because it is not easy to systematically find periodic orbits. This problem only becomes more severe for multiparticle systems. First, there is the high dimensionality of phase space (for example, a two-body system in two space dimensions evolves in an eight-dimensional phase space), and second, there is the intractable proliferation of multiparticle periodic orbits. Consequently, there has been little effort devoted to descriptions or analyses of few-body systems in terms of POT, and no attempt to further develop the theory in such a way as to make it viable to apply to few-body problems. Previously, we began efforts in this direction and derived semiclassical trace formulas for two [6] or more [7] noninteracting identical particles. In this paper, we continue on and consider the effect of weak two-body interactions.

Let us begin by considering the simple (and yet nontrivial) example of two point particles in a one-dimensional infinite square well. If there is no interparticle interaction, the

system is fully integrable, and the fundamental relation between the quantum density of states and classical mechanics is the Berry-Tabor trace formula [8]. The fact that each single-particle energy is conserved automatically means there is a continuous (time-translational) symmetry, and thus the periodic orbits come in one-parameter families that live on two-tori. Interactions destroy the continuous symmetry and therefore break up the periodic orbit families into a discrete set of isolated orbits. The standard Gutzwiller theory can be used *if the interaction is sufficiently strong*. If, however, the particles are weakly interacting, then the system is near-integrable, and although the periodic orbits no longer occur in families that reside on tori, the periodic orbits are not sufficiently isolated, and so the precondition crucial to the derivation of the Gutzwiller trace formula (that the orbits are isolated) is not fulfilled. For weak interactions, the Gutzwiller trace formula thus clearly fails. In principle, this type of problem is not new. Ozorio de Almeida [9] (see also Ref. [10]) considered the perturbation of generically integrable systems, and derived a “uniform approximation” that attempted to smoothly interpolate (divergence-free) between the Berry-Tabor and Gutzwiller limits. Tomsovic, Grinberg, and Ullmo [11] also derived a semiclassical trace formula for two-degree-of-freedom near-integrable and mixed systems. The most important fact to appreciate here is that introducing an interaction is actually a specific example of a more general situation in which there is a breaking of a continuous symmetry. There is a substantial amount of literature on the effect of symmetry breaking on trace formulas [9,11–15], and, in particular, a perturbative theory applicable to any situation in which continuous symmetries are broken has been developed by Creagh in Ref. [12]. The results of this general theory (sometimes referred to as “semiclassical perturbation theory” [1]) can therefore be used to analyze weak interparticle coupling in a two-body system.

*Present address: Department of Physics, Harvard University, Cambridge, MA 02138, USA.

The basic idea is that a calculation to first order in perturbation theory of the actions should be adequate to describe the regime where the periodic orbits are not isolated enough so that the standard Gutzwiller trace formula applies. All members of the continuous family of periodic orbits remain *approximately* periodic if the interaction is weak enough. The basic procedure then is that for a family of unperturbed orbits, we determine the perturbed action after the interaction is turned on. The main step is to expand the action in the exponent to linear order in the perturbation parameter and assume that all other prefactors retain their unperturbed values. If the interaction is sufficiently weak, the only modification to the noninteracting two-body trace formula (see Refs. [6,7]) occurs in the amplitude, which gets modulated by a factor that is (in principle) straightforward to calculate. If the interaction is sufficiently strong, we should use the Gutzwiller trace formula, and for interaction strengths in the intermediate regime, we expect the perturbative theory and the Gutzwiller theory to yield consistent results.

There are many examples of systems we could analyze in order to illustrate the use of the formalism and to give proof-of-concept. Ultimately, we are interested in higher-dimensional systems with unstable dynamics; however, the example we considered above (i.e., a two-body system confined in an infinite square well) is a better starting point, insofar as introducing the formalism. Classically, the one-particle dynamics consist of only *one* primitive orbit, the unperturbed two-body dynamics are scaling, and furthermore, \hbar corrections are not required for the analysis. (The latter would be important for the analysis of certain types of orbits in higher-dimensional billiards.) In fact, the simplicity of the two-body dynamics in the absence of interactions allows for an interesting possibility: semiclassical quantization. The reason is that the main ingredient required in the perturbative analysis is the periodic orbits of the noninteracting two-body system, and since all of these are known in this case, if the effect of the interaction could be computed for all of these orbits, we could then go for a full quantization. Indeed, it is worth the effort, and as will be shown in Sec. III B, the coarse-grained quantum density of states can be accurately reproduced by summing the perturbed contributions for each periodic orbit family. This is quite interesting and important, especially since Creagh's perturbative theory cannot generally be used for the purpose of full quantization [1]. It should also be kept in mind that when a nonscaling interaction is introduced, the resulting two-body system is both nonscaling and nonintegrable. At present, semiclassical quantization of nonintegrable systems (even near-integrable ones) is not viable, and so the periodic orbit quantization of this type of two-dimensional system is quite compelling.

Before starting, we outline the contents of the paper. In Sec. II, we elaborate on the basic ideas we introduced above and give the main formulas. The discussion is somewhat general, but part of it is also geared to the specific example we have in mind to analyze afterwards. We should forewarn readers that Sec. II is concise and assumes familiarity with the results of Ref. [12]. In Sec. III, we apply the ideas and formulas to the example of two identical particles confined in an infinite square well and coupled to each other through a weak Pöschl-Teller two-body interaction. This section is di-

vided into two parts; Sec. III A contains the analytical work and Sec. III B contains the numerics. Finally, in Sec. IV, we conclude the paper with a summary of our results and a brief discussion of possible extensions and future work.

II. SEMICLASSICAL ANALYSIS OF A WEAKLY INTERACTING TWO-BODY SYSTEM

In one dimension, the classical two-body Hamiltonian is

$$H = \frac{p_a^2}{2m} + \frac{p_b^2}{2m} + U(x_a) + U(x_b) + \epsilon V(\mathbf{z}_a, \mathbf{z}_b), \quad (1)$$

where U is a one-body confining potential, and the perturbative term $\epsilon V(\mathbf{z}_a, \mathbf{z}_b)$ is a weak two-body interparticle interaction. The $\mathbf{z}_{a/b}$ are the phase space coordinates of the particles, and ϵ is a continuous parameter.

First, we briefly review the periodic orbit structure for $\epsilon = 0$ (see Ref. [7] for a detailed discussion). Generally speaking, there are two types of periodic orbits in the full two-particle phase space. If both particles evolve on (generally distinct) periodic orbits of the one-particle phase-space with equal period, then the full phase-space periodic orbit is a *dynamical* periodic orbit. In that event, there is a second constant of motion in involution with H . Without loss of generality, this can be chosen to be $J = h_a(\mathbf{z}_a)$, the single-particle Hamiltonian of particle a . It generates time translations of particle a while leaving particle b fixed. There is a corresponding group parameter θ that is conjugate to J and has the dimension of time. For any initial condition on a full phase-space periodic orbit, flows generated by H and J together map out a two-dimensional torus. This means there is a one-parameter degenerate family of periodic orbits. For $\epsilon = 0$, there are also *heterogeneous* periodic orbits in the full phase space, which are periodic orbits that result from one particle executing periodic dynamics while the other particle remains stationary. In particular, suppose that particle a is stationary and particle b evolves dynamically on a periodic orbit. The stationary particle can be anywhere in the billiard, and thus there is a spatial translation symmetry. This implies that the heterogeneous orbits must also occur in continuous families. In addition to E , there is one independent constant of motion J , which (without loss of generality) is the momentum of particle a , that is, $J = p_a$. The corresponding conjugate group parameter is $\Theta = x_a$, where x_a is the spatial translation of particle a . There is an identical contribution to the two-particle resolvent from heterogeneous orbits that derive from particle a evolving on a periodic orbit while particle b is fixed, and in this case, $J = p_b$ and $\Theta = x_b$, where x_b is then the spatial translation of particle b .

If we consider now a typical member of the dynamical periodic orbit family Γ specified by the group parameter θ (denote this orbit by γ_θ), it will still be approximately periodic for $\epsilon \neq 0$, but it will have a modified action. To first order in perturbation theory, the change in action at fixed energy E is (using the theory of Ref. [12])

$$\Delta S_{\Gamma}(E; \theta, \epsilon) \approx -\epsilon \int_{\gamma_{\theta}} V(\mathbf{z}_a(t+\theta), \mathbf{z}_b(t)) dt, \quad (2)$$

where the integral is over an unperturbed orbit γ_{θ} , and the domain of integration is over one period of this orbit. The orbit specified by the parameter θ involves a shift of the initial condition of particle a , that is, $\mathbf{z}_a(t; \theta) = \mathbf{z}_a(t + \theta)$. The amplitude of the unperturbed two-body trace formula (see Ref. [7]) is then multiplied by a ‘‘modulation factor,’’ which is given by (again using the theory of Ref. [12])

$$\mathcal{M}_{\Gamma}(E; \epsilon) = \frac{1}{T_{\Gamma}} \int \exp\left[\frac{i}{\hbar} \Delta S_{\Gamma}(E; \theta, \epsilon)\right] d\theta. \quad (3)$$

If the interaction is absent, then ΔS_{Γ} is zero and the modulation factor is unity. On the other hand, if the interaction is sufficiently strong so that $\Delta S_{\Gamma} \gg \hbar$, then the above integral can be done by stationary phase. Each stationary phase point of the integral corresponds to the initial condition of an isolated orbit in the Gutzwiller limit. For this to be a complete description, we use the analysis outlined above for small interaction strengths and use the isolated orbit analysis for large interaction strengths and expect that there is an intermediate range of interaction strengths in which these analyses are both valid. It is important to note here, however, that this intermediate range cannot be identified at the outset.

As briefly discussed above, there are also contributions to the resolvent from families of heterogeneous orbits when $\epsilon = 0$. Of course, for $\epsilon \neq 0$, there are no such orbits (i.e., these orbits are destroyed and replaced by isolated orbits). However, for weak interactions (i.e., $\epsilon \ll 1$), the Gutzwiller amplitudes of the isolated periodic orbits that replaced the heterogeneous orbit families will again be incorrect and semiclassical perturbation theory should be used to obtain a trace formula with the correct amplitudes. As before, there will be a range of interaction strengths in which this perturbative analysis reproduces the results of the Gutzwiller theory. In the presence of a weak interaction, the heterogeneous periodic orbit γ_x will have a modified action

$$\Delta S_{\Gamma}(E; x, \epsilon) \approx -\epsilon \int_{\gamma_x} V(\mathbf{z}_a = (x_a = x, p_a = 0), \mathbf{z}_b(t)) dt. \quad (4)$$

As before, we integrate over one full period of the unperturbed heterogeneous orbit, which is now the period of the orbit on which particle b evolves. The group parameter x that specifies the particular heterogeneous orbit of the family indicates the position of the stationary particle in the billiard. The modulation factor is then

$$\mathcal{M}_{\Gamma}(E; \epsilon) = \frac{1}{\mathcal{L}} \int_{x_1}^{x_2} \exp\left[\frac{i}{\hbar} \Delta S_{\Gamma}(E; x, \epsilon)\right] dx, \quad (5)$$

where x_1 and x_2 are the positions of the hard walls. The ‘‘group volume’’ $\int dx = (x_2 - x_1) = \mathcal{L}$ is the width of the billiard.

III. EXAMPLE: TWO WEAKLY INTERACTING POINT PARTICLES IN AN INFINITE SQUARE WELL

Consider the one-dimensional single-particle potential

$$U(x) = \begin{cases} 0, & x_1 < x < x_2 \\ \infty & \text{otherwise.} \end{cases} \quad (6)$$

We populate this potential with two particles and introduce a Pöschl-Teller two-body interaction,

$$\epsilon V(|x_a - x_b|) = \epsilon V_0 \operatorname{sech}^2 \kappa(x_a - x_b), \quad (7)$$

where x_a and x_b denote the positions of the two particles, and ϵ is a measure of the interaction strength. (Hereafter, V_0 shall be absorbed into the definition of ϵ , which then has units of energy and can be positive or negative.) This two-body system will generally have mixed dynamics, and for large values of ϵ , the standard Gutzwiller theory can be applied. For small values of ϵ , the Gutzwiller amplitudes become invalid and actually diverge in the limit $\epsilon \rightarrow 0$. Although the tori are destroyed for $\epsilon \neq 0$, the periodic orbits are not sufficiently isolated for small values of ϵ since their perturbed actions differ by less than \hbar .

A. Semiclassical analysis

Consider first the noninteracting case ($\epsilon = 0$). The smooth average density of states can be obtained simply from the convolution identity

$$\bar{\rho}_2(E) = \bar{\rho}_1(E) * \bar{\rho}_1(E) = \frac{m\mathcal{L}^2}{2\pi\hbar^2} - \sqrt{\frac{2m}{E}} \frac{\mathcal{L}}{2\pi\hbar} + \frac{1}{4} \delta(E), \quad (8)$$

where we have used the formula

$$\bar{\rho}_1(E) = \frac{1}{2} \left[\frac{1}{\sqrt{E_0 E}} - \delta(E) \right], \quad (9)$$

and $E_0 \equiv \pi^2 \hbar^2 / 2m\mathcal{L}^2$ is the ground-state energy of the one-body system. [Note that $\mathcal{L} = (x_2 - x_1)$ is the width of the well.] In Eqs. (8) and (9), the δ -function correction does not actually contribute to the density of states, but rather to any integrated quantity for which the density of states is part of the integrand [the most common example is the smooth part of the cumulative density of states $\bar{N}(E) = \int_0^E \bar{\rho}(\xi) d\xi$]. This correction has been identified as belonging to the one-particle Weyl expansion [see, for example, Eq. (4.141) of Ref. [1]], and will be important in a subsidiary calculation described below.

As briefly described in Sec. II, there are two contributions to the oscillatory part of the density of states. One comes from the dynamical periodic orbits, and the other from the heterogeneous periodic orbits. The dynamical periodic orbits consist of both particles executing independent single-particle motions on some repetition of the primitive periodic orbit. If a particle is launched at x_1 , and the repetition index of the orbit is n , then the position of a particle as a function of time (i.e., the configuration space periodic orbit) is

$$x(t;n) = \sum_{j=0}^{(2n-1)} \left[X_j + (-1)^j v \left(t - \frac{jT}{2n} \right) \right] G_{T/2n} \left(t - \frac{jT}{2n} \right), \quad (10)$$

where X_j is x_1 or x_2 when j is even or odd, respectively, v is the speed of the particle, T is the period of the orbit, and the gate function is defined as

$$G_\mu(t-\nu) = \begin{cases} 0, & t < \nu \\ 1, & \nu < t < \mu + \nu \\ 0, & t > \mu + \nu. \end{cases} \quad (11)$$

Suppose that particles a and b are on the n_a th and n_b th repetition of the primitive orbit. Using the results of Ref. [7], the contribution of the dynamical periodic orbits to the two-particle resolvent is

$$\tilde{g}_2^d(E) = -i\pi \sum_{n_a=1}^{\infty} \sum_{n_b=1}^{\infty} \frac{\exp i \left[2\pi \sqrt{(n_a^2 + n_b^2)E/E_0} - \frac{\pi}{4} \right]}{[(n_a^2 + n_b^2)E_0^3 E]^{1/4}}. \quad (12)$$

The heterogeneous orbits occur when one particle is fixed inside the well while the other particle evolves on a periodic orbit. Since the stationary particle can be anywhere in the well, there is a translation symmetry that is generated by the momentum. Using the results of Ref. [7], heterogeneous orbits make the following contribution to the two-particle resolvent:

$$\tilde{g}_2^h(E) = -i\pi \sum_{n=1}^{\infty} \frac{\exp i \left(2n\pi \sqrt{E/E_0} - \frac{\pi}{4} \right)}{(n^2 E_0^3 E)^{1/4}}. \quad (13)$$

Note that both Eqs. (12) and (13) are $O(1/\hbar^{3/2})$, and have identical energy prefactors $O(1/E^{1/4})$, which is generally true for orbits that occur in one-parameter families. The standard semiclassical approximation for the oscillatory part of the resolvent, that is, the leading-order semiclassical trace formula, is the sum of Eqs. (12) and (13). Numerically, this yields a set of peaks at the positions of the quantum two-particle spectrum *and* a spurious set of peaks at the positions of the one-particle spectrum. There is, however, a ‘‘boundary correction’’ to Eq. (13). This term is not relevant for our purposes, but we should at least mention the subtle way it emerges. This correction arises from the ‘‘grazing’’ heterogeneous orbits, which are those orbits for which the stationary particle resides at the wall of the square well. These orbits represent the boundary of the heterogeneous orbit family and are of course not isolated. Mathematically, the correction to Eq. (13) arises as an end-point correction to the trace integral over the heterogeneous orbit family, while the leading-order contribution [Eq. (13)] comes from the stationary phase points of the integrand. The correction term itself happens to be exactly the trace formula for a single particle in the square well, accompanied by an overall minus sign [i.e., $-\tilde{\rho}_1(E)$], and is $O(1/\hbar)$. We note that this correction is identical to the boundary correction for the two-dimensional square billiard

[see Eq. (2.187) of Ref. [1]]. When we include this term with the leading-order heterogeneous term, it exactly cancels the spurious peaks mentioned above. A similar situation occurs in the case of one particle in an equilateral triangle billiard (see Sec. 6.1.2 of Ref. [1]).

We now examine each contribution to the density of states for $\epsilon \neq 0$. The Thomas-Fermi (TF) term, that is, the leading-order term of the average density of states, can be computed from the inverse Laplace transform of the classical two-particle partition function $Z_2^{\text{cl}}(\beta) = \frac{1}{2(2\pi\hbar)^2} \int d\mathbf{q} \int d\mathbf{p} \exp[-\beta\mathcal{H}(\mathbf{q}, \mathbf{p})]$. The integral over momentum $\mathbf{p} = (p_a, p_b)$ is trivial, and the remaining integral over the coordinates $\mathbf{q} = (x_a, x_b)$ can be transformed to a one-dimensional integral after a change of variables to center-of-mass and relative coordinates: $X = (x_a + x_b)/2$, $x = (x_a - x_b)$. Under the inverse Laplace transform, this reduces to

$$\bar{\rho}_2(E; \epsilon, \kappa) = \frac{m\mathcal{L}}{2\pi\hbar^2} \int_0^{\mathcal{L}} \Theta(E - \epsilon \operatorname{sech}^2 \kappa x) dx, \quad (14)$$

where $\Theta(\dots)$ in Eq. (14) is a step function. Due to the properties of the integrand, the TF term is a constant, $m\mathcal{L}^2/2\pi\hbar^2$ for $E > \epsilon$. When $0 \leq E \leq \epsilon$, the TF term is a complicated function of E , but this range of E is unimportant for the calculations we pursue here.

For the oscillatory part of the density of states, we must determine the perturbed actions for each family of *unperturbed* orbits. For dynamical orbits, the particles are generally out of phase, and the unperturbed orbits are $x_a(t+\theta) = x(t+\theta; n_a)$ and $x_b(t) = x(t; n_b)$. Then, from Eqs. (2) and (7),

$$\begin{aligned} \Delta S_{\Gamma}(E; \theta, \epsilon, \kappa) &\approx -\epsilon \int_{\gamma_\theta} V(x_a(t+\theta), x_b(t)) dt \\ &= -\epsilon \int_0^T \operatorname{sech}^2 \kappa [x_a(t+\theta) - x_b(t)] dt. \end{aligned} \quad (15)$$

The above integral splits into $2(n_a + n_b)$ intervals, each of which must be evaluated separately. To evaluate the integral, the distance function $\mathcal{D}_{ab}(t; \theta) = x_a(t+\theta) - x_b(t)$ should be calculated on θ intervals of size $T/2n_a n_b$; the reason is that particle a reverses direction at $j_a T/2n_a$ ($j_a = 1, 2, 3, \dots, 2n_a$), whereas particle b reverses direction at $j_b T/2n_b$ ($j_b = 1, 2, 3, \dots, 2n_b$), and thus the distance function changes discontinuously at values of θ that are integer multiples of $\min\{|j_a T/2n_a - j_b T/2n_b| : j_a n_b - j_b n_a \neq 0\} = T/2n_a n_b$, or more precisely $\mathcal{D}_{ab}(t; \theta)$ changes discontinuously at $\theta_j = jT/2n_a n_b$, where $j = 1, 2, 3, \dots, 2n_a n_b$. After careful integration of Eq. (15) using Eq. (10) in the argument of the secant function, we find, by induction, the action shift, for $\ell T/2n_a n_b \leq \theta \leq (\ell+1)T/2n_a n_b$, $\ell = 0, 1, 2, 3, \dots, (2n_a n_b - 1)$, is

$$\begin{aligned} \frac{\Delta S_\Gamma(E; \theta, \epsilon, \kappa)}{\hbar} = & -\frac{2\epsilon v_a}{\hbar \kappa (v_a^2 - v_b^2)} \\ & \times \sum_{k=0}^{(n_a-1)} \left[\tanh \kappa \left(v_b \theta + \frac{(k-\ell)\mathcal{L}}{n_a} \right) \right. \\ & \left. + \tanh \kappa \left(-v_b \theta + \frac{(k+1+\ell)\mathcal{L}}{n_a} \right) \right] \\ & + \{a \leftrightarrow b\}, \end{aligned} \quad (16)$$

where $v_{alb} = \sqrt{2E_{alb}/m}$. The energies of the particles are such that the periods of the unperturbed orbits are the same: $E_{alb} = n_{alb}^2 E / (n_a^2 + n_b^2)$. (Of course, $E_a + E_b = E$.) The physical meaning of the terms involving \mathcal{L} will become clear after the asymptotic analysis below. As we shall see, each of these terms is an initial coordinate of particle a on an isolated orbit of the Gutzwiller limit. As deduced above, the distance function and therefore $\Delta S_\Gamma(\theta)$ has a different functional form in each of the $2n_a n_b$ θ intervals. However, the range of the action shifts turns out to be the same for all intervals. Thus, it is sufficient to compute the action shift for one interval (for instance, the first interval) and then use the multiplicative factor $2n_a n_b$ when computing the modulation factor \mathcal{M}_Γ , which is then found by integrating over θ ,

$$\mathcal{M}_\Gamma(E; \epsilon, \kappa) = \frac{2n_a n_b}{T_\Gamma} \int_0^{T_\Gamma/2n_a n_b} \exp \left[\frac{i}{\hbar} \Delta S_\Gamma(E; \theta, \epsilon, \kappa) \right] d\theta, \quad (17)$$

where $\Gamma = (n_a, n_b)$, ΔS_Γ is given by Eq. (16), and the common period $T_\Gamma = T_{n_a}(E_a) = T_{n_b}(E_b) \equiv T(E) = \pi \hbar \sqrt{(n_a^2 + n_b^2)/E_0 E}$.

If the unperturbed dynamical orbit results from both particles evolving on the same orbit of the one-particle phase space (i.e., $n_a = n_b = n$), the distance function changes discontinuously at integer multiples of $T/2n$. Then, the integral in Eq. (15) splits into $4n$ intervals, and again using Eq. (10) in the argument of the secant function, we find, by induction,

$$\begin{aligned} \frac{\Delta S_\Gamma(E; \theta, \epsilon, \kappa)}{\hbar} = & -\frac{2n\epsilon}{\hbar} \left[\left(\frac{T_\Gamma}{2n} - \theta \right) \operatorname{sech}^2(\kappa v \theta) \right. \\ & \left. + \frac{1}{\kappa v} \tanh(\kappa v \theta) \right] \end{aligned} \quad (18)$$

for $0 \leq \theta \leq T_\Gamma/2n$, where $v = \sqrt{E/m}$. Similarly, for the other θ intervals. The complete modulation factor is then

$$\mathcal{M}_\Gamma(E; \epsilon, \kappa) = \frac{2n}{T_\Gamma} \int_0^{T_\Gamma/2n} \exp \left[\frac{i}{\hbar} \Delta S_\Gamma(E; \theta, \epsilon, \kappa) \right] d\theta, \quad (19)$$

where $\Gamma = (n, n)$, the common period $T_\Gamma = T_n(E_a) = T_n(E_b) \equiv T(E) = n\pi \hbar \sqrt{2/E_0 E}$, and ΔS_Γ is as given in Eq. (18). The modulation [Eq. (17) or Eq. (19)] is then inserted as a multiplicative factor in the summation of Eq. (12). Finally, the contribution of the dynamical orbits to the oscillatory part of the density of states is $\tilde{\rho}_2^d(E; \epsilon, \kappa) = -\frac{1}{\pi} \operatorname{Im}\{\tilde{g}_2^d(E; \epsilon, \kappa)\}$, and thus

$$\begin{aligned} \tilde{\rho}_2^d(E; \epsilon, \kappa) = & \sum_{n_a=1}^{\infty} \sum_{n_b=1}^{\infty} \frac{1}{[n_\Gamma^2 E_0^3 E]^{1/4}} \left[\operatorname{Re}\{\mathcal{M}_\Gamma(E; \epsilon, \kappa)\} \right. \\ & \times \cos \left(S_\Gamma(E) - \frac{\pi}{4} \right) + \operatorname{Im}\{\mathcal{M}_\Gamma(E; \epsilon, \kappa)\} \\ & \left. \times \sin \left(S_\Gamma(E) - \frac{\pi}{4} \right) \right], \end{aligned} \quad (20)$$

where $\Gamma = (n_a, n_b)$, $n_\Gamma^2 = (n_a^2 + n_b^2)$, and $S_\Gamma(E) = 2\pi \sqrt{n_\Gamma^2 E/E_0}$.

In the limit $\Delta S_\Gamma \gg \hbar$, we can analyze the modulation integrals by stationary phase. As examples, consider $\Gamma = (1, 1)$ and $\Gamma = (2, 1)$. In the former, using the modulation factor (19), there are two contributions. These have phases of $\pm\pi/4$ relative to the noninteracting case and have relative amplitudes $O(\sqrt{\hbar})$. The two stationary phase points $\theta=0$ and $\theta=T/2$ correspond physically to the situations in which the two particles are initially in phase and $T/2$ out of phase, respectively. For $T/2 \leq \theta \leq T$, there are also two stationary phase points $\theta=T/2$ and $\theta=T$, but these are extraneous since these points describe the same situations as before (i.e., $\theta=0$ and $\theta=T$ indicate that both particles are initially at x_1). The corresponding shifts in the action are $\Delta S(0) = -\epsilon T$ and $\Delta S(T/2) = -\epsilon T \tanh(\kappa \mathcal{L}) / \kappa \mathcal{L}$, respectively. For $\Gamma = (2, 1)$, using Eq. (17), there are nine critical points $\theta_w = wT/8$, $w = 0, 1, 2, \dots, 8$. These stationary phase points do not all describe unique initial conditions, in the sense that several of them correspond to the same initial conditions. Actually, these points correspond physically to one of *four* situations: (i) both particles are initially at x_1 with $p_a > 0$ ($\theta=0, T/2$, and T); (ii) particle b is at x_1 while particle a is at the center of the well with $p_a > 0$ ($\theta=T/8$ and $5T/8$); (iii) same as (ii) except $p_a < 0$ ($\theta=3T/8$ and $7T/8$); (iv) the particles are at opposite sides of the well ($\theta=T/4$ and $3T/4$). In cases (ii) and (iii), the particles are separated by a distance $\mathcal{L}/2$, whereas in case (iv), the particles are separated by a distance \mathcal{L} . This analysis implies that the periodic orbit family $\Gamma = (2, 1)$ is broken up and replaced by four isolated orbits.

More generally, if $n_a \neq n_b$, there are $(4n_a n_b + 1)$ critical points $\theta_w = wT/(4n_a n_b)$, where $w = 0, 1, 2, \dots, 4n_a n_b$. If $n_a = n_b = n$, there are $(2n+1)$ critical points $\theta_w = wT/2n$, where $w = 0, 1, 2, \dots, 2n$. In all cases, the action shifts are obtained by substituting each stationary phase point into Eqs. (16) and (18). As in the specific examples given above, the complete set of stationary phase points do not all describe unique initial conditions. Many of the stationary phase points are degenerate in the sense that they correspond to the same initial conditions. The symmetric periodic orbit families ($n_a = n_b$) are always broken up into *two* isolated orbits (corresponding to situations in which the particles either both begin at x_1 or begin at opposite sides of the square well), and the nonsymmetric periodic orbit families ($n_a \neq n_b$) are broken up into $2n_a n_b$ isolated orbits (corresponding to situations in which the particles are initially separated by integer multiples of $\mathcal{L}/n_a n_b$). These results are consistent with Birkhoff's theorem, which states that any smooth perturbation results in an *even* number of isolated orbits, of alternating stability. Note that the number of critical points increases with the length of

the orbits. This implies that families having smaller actions break into relatively fewer isolated orbits than families having larger actions, which are replaced by many more isolated orbits.

We could imagine that there exists a range of interaction strengths where the perturbation is small enough to justify the use of semiclassical perturbation theory while nevertheless $\Delta S \gg \hbar$. We would then still use the formalism of this paper for small interaction strengths and use the isolated orbit analysis for large interaction strengths and expect that there is an intermediate regime in which both analyses are valid.

For heterogeneous orbits, upon adding an interaction, the specific property that one of the particles is stationary while the other evolves with all of the energy will no longer be true, but it is still necessary to smoothly interpolate between the cases in which the translation symmetry exists and the case for which this symmetry is broken. To first order in perturbation theory, the change in action (at fixed energy E), for a typical member γ_x of the heterogeneous orbit family Γ , is

$$\Delta S_\Gamma(E; x, \epsilon) \approx -\epsilon \int_{\gamma_x} V(x_1 + x, x_b(t)) dt. \quad (21)$$

In the above formula, the group parameter x is the displacement from x_1 (the position of the left wall), and $0 \leq x \leq \mathcal{L}$. As before, we integrate over one period of the orbit family. In this case, this is the period of the evolving particle T . If the evolving particle is on the n th repetition of the primitive orbit, then the shift in the action is

$$\Delta S_n(E; x, \epsilon, \kappa) = \frac{2n\epsilon}{\kappa v} \{ \tanh \kappa [x + (x_1 - x_2)] - \tanh \kappa x \}, \quad (22)$$

where $v = \sqrt{2E/m}$. The modulation factor for the heterogeneous orbits is then

$$\mathcal{M}_n(E; \epsilon, \kappa) = \frac{1}{\mathcal{L}} \int_0^{\mathcal{L}} \exp \left[\frac{i}{\hbar} \Delta S_n(E; x, \epsilon, \kappa) \right] dx. \quad (23)$$

[Note the group volume $\int_0^{\mathcal{L}} dx = \mathcal{L} = (x_2 - x_1)$.] The modulation factor in Eq. (23) is now included as a multiplicative factor in the summation of Eq. (13). Thus, the contribution of the heterogeneous orbits to the oscillatory part of the density of states is $\tilde{\rho}_2^h(E; \epsilon, \kappa) = -\frac{1}{\pi} \text{Im} \{ \tilde{g}_2^h(E; \epsilon, \kappa) \}$, that is,

$$\begin{aligned} \tilde{\rho}_2^h(E; \epsilon, \kappa) &= \sum_{n=1}^{\infty} \frac{1}{(n^2 E_0^3 E)^{1/4}} \left[\text{Re} \{ \mathcal{M}_n(E; \epsilon, \kappa) \} \cos \left(S_n(E) - \frac{\pi}{4} \right) \right. \\ &\quad \left. + \text{Im} \{ \mathcal{M}_n(E; \epsilon, \kappa) \} \sin \left(S_n(E) - \frac{\pi}{4} \right) \right], \quad (24) \end{aligned}$$

where $S_n(E) = 2n\pi\sqrt{E/E_0}$.

For large values of ϵ , we can again analyze the modulation integral by stationary phase. In this case, we get only one contribution since there is only one stationary phase point $x = (x_1 + x_2)/2$, which is at the center of the well. Thus, after the interaction is turned on, each heterogeneous orbit

family is destroyed and replaced by a single isolated orbit. The correction that arises from the perturbed contribution of the ‘‘grazing’’ heterogeneous orbits is not generally important for quantization. Including this correction term is crucial only if we are interested in perturbed levels of the two-body system whose unperturbed counterparts coincide with a level of the one-body spectrum. (These degeneracies are quite rare; for example, for $E < 1000$, there are only 10 such levels.) Otherwise, the leading-order semiclassical trace formulas are sufficient. Therefore,

$$\tilde{\rho}_2^{\text{sc}}(E; \epsilon, \kappa) = \tilde{\rho}_2^h(E; \epsilon, \kappa) + \tilde{\rho}_2^d(E; \epsilon, \kappa). \quad (25)$$

B. Numerics

For numerical purposes, we define a semiclassical coarse-grained density of states using the Gaussian-convolved trace formula (GCTF)

$$\begin{aligned} \tilde{\rho}_\sigma^{\text{sc}}(E; \epsilon, \kappa) &\approx \sqrt{2\pi\sigma} \sum_\Gamma \exp \left[\frac{-2\sigma^2 T_\Gamma^2(E)}{4\hbar^2} \right] A_\Gamma(E) \\ &\quad \times \text{Im} \left\{ i \mathcal{M}_\Gamma(E; \epsilon, \kappa) \exp \left[i \left(S_\Gamma(E) - \frac{\pi}{4} \right) \right] \right\}, \quad (26) \end{aligned}$$

which [upon adding the Gaussian-convolved Thomas-Fermi term $\tilde{\rho}_\sigma(E; \epsilon, \kappa)$] is the semiclassical approximation to the exact quantum Gaussian coarse-grained density of states (CGDOS),

$$\rho_\sigma(E; \epsilon, \kappa) = \rho_2(E; \epsilon, \kappa) * G_\sigma(E) = \sum_n \exp \left[-\frac{(E - E_n)^2}{2\sigma^2} \right], \quad (27)$$

which is a set of Gaussian spectral lines (of width $\sqrt{2}\sigma$) centered at each energy of the quantum two-body spectrum $\{E_n : n \in \mathbb{N}\}$. In Eq. (26), Γ refers to a dynamical or heterogeneous orbit family, $T_\Gamma(E)$ is its period, and $A_\Gamma(E)$ is its *unperturbed* amplitude [i.e., the amplitudes of Eqs. (20) and (24) when $\mathcal{M}_\Gamma = 1$]. The sum in Eq. (26) derives from convolving the perturbed trace formulas with an *unnormalized* Gaussian function $G_\sigma(E) = \exp(-E^2/2\sigma^2)$. More precisely, Eq. (26) is obtained from an asymptotic analysis of the convolution integral,

$$\begin{aligned} \tilde{\rho}_\sigma^{\text{sc}}(E; \epsilon, \kappa) &= \tilde{\rho}_2^{\text{sc}}(E; \epsilon, \kappa) * G_\sigma(E) \\ &= -\frac{1}{\pi} \text{Im} \{ \tilde{g}_2^{\text{sc}}(E; \epsilon, \kappa) * G_\sigma(E) \}. \quad (28) \end{aligned}$$

The convergence of the sums in Eqs. (20) and (24) is enforced through an exponential damping factor [$\exp(-\sigma^2 \alpha L_\Gamma^2 / 8E)$] in the amplitude. The parameter σ is the variance of the Gaussian, $\alpha = 2m/\hbar^2$, and L_Γ is the length of the *unperturbed* periodic orbit family Γ . If all orbits with length $L < L_{\text{max}}$ are included, then there exists a set of energy values $E < E_{\text{max}}$ for which the exponential factor falls below some threshold parameter δ . This condition immediately gives a simple relation between all the relevant numerical parameters,

$$L_{\max} = \frac{2\sqrt{-2E_{\max} \ln(\delta)}}{\sigma\sqrt{\alpha}}. \quad (29)$$

(Note that $0 < \delta < 1$, and that σ has units of energy and thus L_{\max} has units of length.) For $L_{\Gamma} > L_{\max}$ and $E < E_{\max}$, all terms are exponentially smaller than δ , and are thus numerically insignificant. The numerical parameter δ is an amplitude cutoff. The largest errors are in the vicinity of E_{\max} where there are contributions $O(\delta)$ that have been excluded. For all other values of $E < E_{\max}$, the excluded terms are exponentially smaller than δ . So, we truncate Eq. (26) and include all orbits with length $L < L_{\max}$. We first specify E_{\max} , σ , and δ , and then L_{\max} is determined from the condition that all orbits with length $L > L_{\max}$ have amplitudes smaller than δ [Eq. (29)].

Numerical computation of the lowest 500 quantum energies for each irreducible representation (converged to near machine accuracy) was achieved using the Lanczos method for real symmetric matrices [16]. The Lanczos iteration entails successive applications of the Hamiltonian operator to an arbitrary state vector represented in a suitable basis. In our computations, symmetry adaptation of a simple product basis (i.e., the eigenbasis of the unperturbed system) was employed to reduce the size of the state vectors by a factor of 4 (in comparison to the unadapted basis). The precise means of implementing a symmetry-adapted basis without explicit construction of the Hamiltonian matrix will not be described here. Lanczos iteration determines a tridiagonal representation of the Hamiltonian whose eigenvalues are efficiently extracted via bisection [17]. However, it is well known that the Lanczos method produces spurious eigenvalues. For example, converged eigenvalues appear as multiply degenerate (or near degenerate) with increasing degeneracy as the number of iterations increases. While such spurious degeneracy is easily identified and eliminated, spurious nondegenerate eigenvalues also appear. These can be eliminated by constructing the associated eigenvector using one-step inverse iteration. We will not describe this procedure here, but we should mention that this means of eliminating spurious eigenvalues is different from that described in Ref. [16].

In Fig. 1, we compare the exact CGDOS (27) with its semiclassical approximation as evaluated from the GCTF (26) for $\epsilon = 1/8, 1/4$, and $1/2$ ($\kappa = 1$). In our calculations, we considered the energy window $[E_{\min}, E_{\max}] = [50, 75]$ but two smaller windows are displayed here so that more detail may be discerned. The prescribed numerical parameters $\delta = 10^{-6}$, $\sigma = 1/40 = 0.025$ (and thus $L_{\max} = 1160\mathcal{L}$). For all numerical calculations in this paper, $m = 1/2$, $\hbar = 1$, $x_1 = 0$, and $x_2 = \pi$ so that $\mathcal{L} = \pi$ and $E_0 = 1$. It is clear from these representative calculations that the GCTF accurately reproduces the exact CGDOS when ϵ is small (e.g., $\epsilon = 1/8$), and can fail as ϵ is increased. The failure, however, is not as simple as one might expect. Evidently, the spectral lines corresponding to perturbed energies whose unperturbed counterparts are ‘‘symmetric energies’’ become erroneous, whereas the spectral lines corresponding to perturbed energies whose unperturbed counterparts are ‘‘nonsymmetric energies’’ are correct for moderately large values of ϵ . For example, the evolution

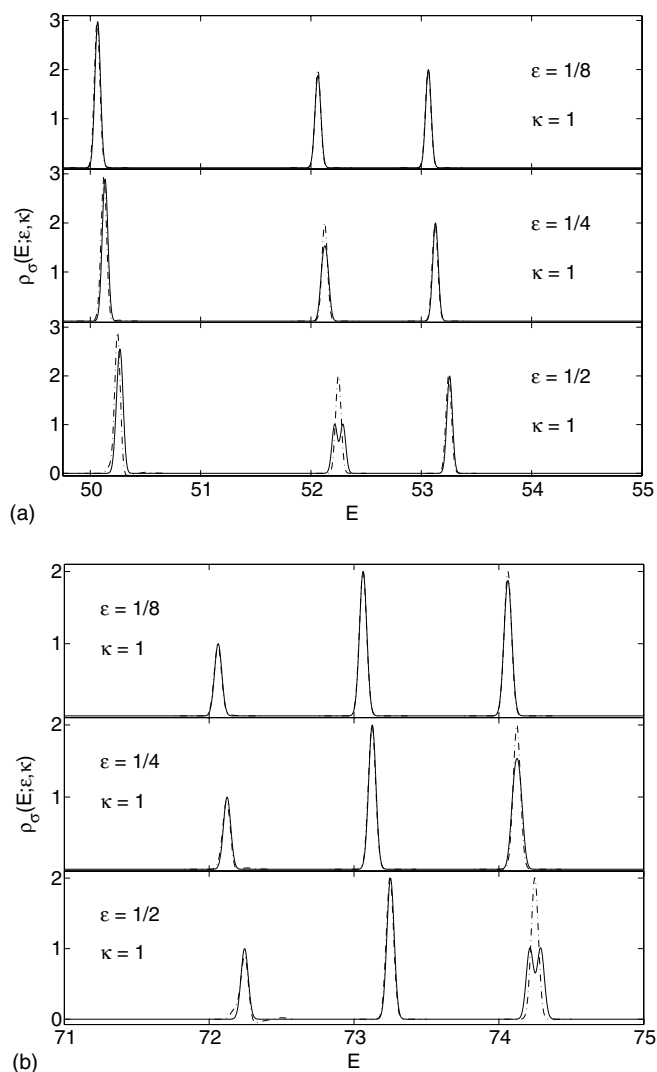


FIG. 1. The coarse-grained density of states (CGDOS) in the presence of a weak medium-range ($\kappa = 1$) interparticle interaction. Two small energy windows (chosen arbitrarily) are shown here and are representative. The solid line is the exact quantum CGDOS [Eq. (27)], and the dashed-dotted line is the semiclassical CGDOS obtained from the Gaussian-convolved trace formula (26). The amplitude cutoff $\delta = 10^{-6}$, and the variance $\sigma = 1/40 = 0.025$.

of the (symmetric) singlet energy $E = 6^2 + 6^2 = 72$ under perturbation clearly becomes incorrect as the interaction strength increases; the spectral line produced by the GCTF differs from the Gaussian line of the exact CGDOS. The same type of error occurs for the $E = 50$ triplet, which experiences a splitting under perturbation as the initially degenerate energies shift by differing amounts. This splitting is of course too fine to observe directly from the CGDOS, but again there is a clear difference (when $\epsilon = 1/2$) between the spectral lines produced by quantum and semiclassical mechanics. In contrast, the ‘‘coarse-grained’’ evolution of the $E = 53$ doublet or the $E = 65$ quartet (not shown in Fig. 1) under perturbation is correctly reproduced by semiclassics. The difference between the triplet and the doublet (or quartet) is that a symmetric energy $E = 5^2 + 5^2 = 50$ is one of the unperturbed triplet energies, whereas none of the unper-

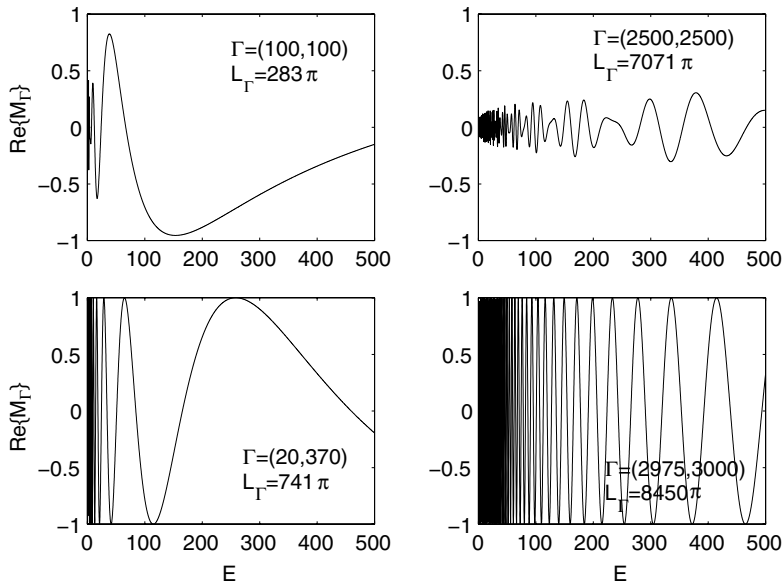


FIG. 2. The real part of the modulation factor [Eq. (17) or Eq. (19)] for orbit families $\Gamma = (n_a, n_b)$ perturbed by a long-range repulsive interaction ($\epsilon=0.1$ and $\kappa=1/\mathcal{L}=1/\pi$).

turbed doublet or quartet energies in question are symmetric energies. It is not obvious to us why the formalism fails for certain states and not others, but nevertheless that is the observation. Notice also that in some cases there are obvious splittings that are not reproduced by the perturbed trace formulas. Good agreement between quantum and semiclassical results can be achieved by increasing the coarse-graining (i.e., the value of σ). We will say more about splittings and the behavior of the multiplet states under perturbation later on.

At this point, it is illuminating to study in more detail the evolution of the singlet states, that is, the states that are non-degenerate when $\epsilon=0$. From quantum perturbation theory, we know the energies of these states are simply shifted away from their unperturbed values for $\epsilon \neq 0$. Semiclassically, the same behavior ensues (see Fig. 1) as a result of the action shifts discussed in the previous section. We now want to get more precise information; we want to obtain numerical estimates of the actual perturbed energies for some small value of ϵ . Generally speaking, each spectral line generated by the GCTF that is isolated and has height equal to 1 is a Gaussian line whose maximum (=1) occurs at a position along the energy axis to be identified with a semiclassical energy [20]. Semiclassical energies obtained in this way can be computed to a specified accuracy by evaluating the GCTF on energy windows of appropriate size. We start with an energy window that encloses the entire peak of interest and then systematically refine the size of the window until the position of the peak maximum has been located to the desired accuracy. The convergence can be checked by including many orbits with length greater than L_{\max} and verifying that the position of the peak maximum does not change within the specified accuracy. The energies will be given to $O(10^{-5})$. In the following calculations, the amplitude cutoff $\delta=10^{-10}$. It is important to keep in mind that the exact positions of peak maxima will generally depend on the specific choice of the parameter σ . The relative numerical importance of the Thomas-Fermi term also depends on the specific choice of σ . The smaller the value of σ , the less important $\bar{\rho}_2(E; \epsilon, \kappa)$

becomes and vice versa. However, the leading-order TF term only affects the height of the peak maximum and not its position along the energy axis.

Although we have complete freedom in specifying the variance σ , it should not be chosen too small since this will require that L_{\max} must be quite large. This is, of course, impractical, but there is a more fundamental problem; Creagh's perturbative theory is known to fail for long orbits [12]. Besides, the error introduced by including long orbits does not arise from the semiclassical approximation alone. The GCTF itself becomes less accurate when long orbits are included. The reason is that the modulation factor for long orbits is highly oscillatory for low-lying values of E (see, for example, Figs. 2 and 3). The asymptotic analysis of the convolution integral [Eq. (28)] that yields the GCTF (26) assumes that the *perturbed* amplitude of the trace formula is a smooth slowly varying function of E . (Note that the perturbed amplitude includes the modulation factor \mathcal{M}_Γ .) To leading order, the amplitude can then be taken outside the convolution integral since it is approximately constant on an interval of size σ . If the modulation factor is oscillating rapidly in some energy range (as it does for long orbits), this assumption is no longer valid. However, the interest here is not in how the perturbative procedure breaks down when long orbits are included. The important point is that the $\epsilon \neq 0$ GCTF does not converge to the exact quantum coarse-grained level density as $L_{\max} \rightarrow \infty$. Nevertheless, we can still choose a moderately small value for σ and obtain a good estimate of the energy shift. Note that the variance σ must still be small enough to resolve individual levels. For the analysis of the singlet states (which are sufficiently isolated), the value $\sigma=0.1$ is a good compromise that satisfies both requirements. The trace formulas are exact for $\epsilon=0$ and any numerical errors arise exclusively from the approximations made in obtaining the GCTF (26). In the unperturbed case, the amplitude $A_\Gamma(E) \sim E^{-1/4} \forall \Gamma$, which is approximately constant on intervals of size σ for $E \geq 1$. Since all orbit families have this energy dependence in their amplitudes, the asymptotic analysis of the convolution integral is accurate for all orbits, and be-

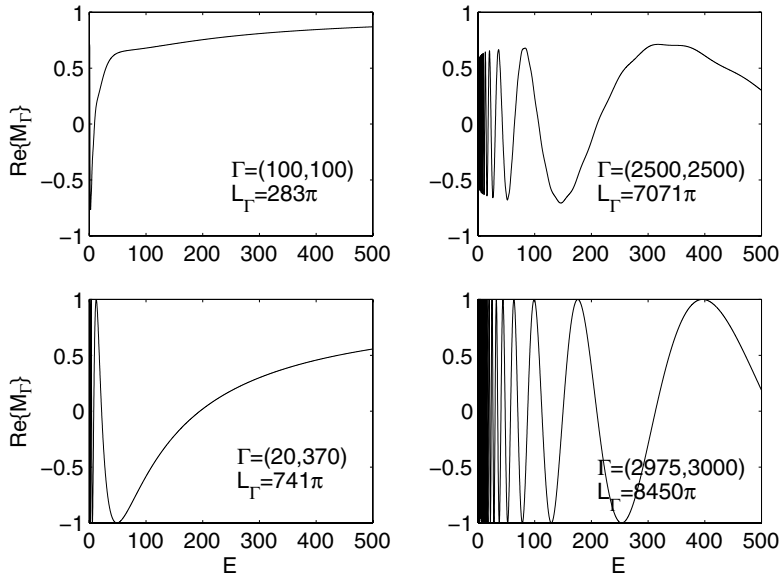


FIG. 3. Same as Fig. 2, except the orbit families $\Gamma=(n_a, n_b)$ are perturbed by a short-range repulsive interaction ($\epsilon=0.1$ and $\kappa=\mathcal{L}=\pi$).

comes more accurate as $\sigma \rightarrow 0$. So, as $\sigma \rightarrow 0$ and $L_{\max} \rightarrow \infty$, the sum converges to the exact quantum result (27). Examination of the $\epsilon=0$ singlet lines reveals that, for $25 \leq E \leq 100$, the errors inherent in the GCTF are $O(10^{-5})$ when $\sigma=0.1$. (For $E > 100$, there is slow, but steady, improvement.) Numerical analysis of the $\epsilon \neq 0$ GCTF confirms that smaller values of σ yield *less* accurate results, as expected.

It should be emphasized that corrections to the Thomas-Fermi term are not negligible and these introduce an additional error. (To the level of precision considered here, the smooth term does change across the width of a peak even if that peak is narrow.) A precise determination of this error requires a separate numerical analysis of the smooth average density of states, but since the interest here is only to estimate the energy shift, no further analysis of the smooth term will be undertaken. An estimate of the error can be inferred from the unperturbed case, where the ‘‘perimeter correction’’ [the second term of Eq. (8)] causes changes in $\bar{\rho}_2(E)$ of $O(10^{-4})$ across energy windows of size $\sigma \sim 0.1$ when $10 \leq E \leq 100$ and of $O(10^{-5})$ or less when $E \geq 100$. This sug-

gests that for the perturbed case we should expect errors of at least the same order from neglected corrections to the Thomas-Fermi term.

In Tables I–IV, the shifts of five low-lying singlets (excluding the first three singlets) plus one higher-lying singlet are given for $\epsilon = \pm 0.1$. In each case, the data were generated using $L_{\max} = 1000\mathcal{L}$ and $\sigma = 0.1$. This amounts to using $N_d = 98\,095$ dynamical orbit families and $N_h = 500$ heterogeneous orbit families. A consistent length truncation requires that both trace formulas [Eqs. (20) and (24)] include only orbits with length $L \leq L_{\max}$. It is incorrect to simply specify an upper truncation limit for the sums. Since the dynamical orbits proliferate much more rapidly than the heterogeneous orbits, that is, $N_d(L) \gg N_h(L)$, many more of the former must be included in the truncated sums. For large L , the role of the heterogeneous orbits is relatively minor, but nevertheless important since their contribution ensures the spectral lines have the correct shape and height.

As the numerics demonstrate, for singlet states of the unperturbed system with energy $25 \leq E \leq 500$, the GCTF gives

TABLE I. Perturbed energies for six singlet states of the unperturbed two-body system. The parameters $\epsilon=0.1$ and $\kappa=1/\mathcal{L}=1/\pi$. This choice of κ corresponds to an interaction that is long-range with respect to the size of the well. The first column specifies the state number in the symmetric irrep (i.e., the n th state of the symmetric irrep), and the second and third columns give the exact unperturbed and perturbed quantum energies, respectively. The fourth and fifth columns are the energies obtained from quantum and semiclassical perturbation theory. The difference between the exact quantum and semiclassical values is given in the last column. The difference between exact and quantum perturbation theory $\Delta_n^{\text{qm}} = E_n - E_n^{\text{qm}} = 0.000\,03$ for each given n . For comparison, if $\sigma=0.05$ in Eq. (26) (so that longer orbits are less suppressed), then $E_{20}^{\text{sc}} = 98.086\,57$; the semiclassical error ($\Delta_{20}^{\text{sc}} = 0.000\,27$) is larger, but the semiclassical energy shift is unchanged to $O(10^{-3})$.

n	$E_n^{(0)}$	E_n	E_n^{qm}	E_n^{sc}	Δ_n^{sc}
7	32	32.08709	32.08713	32.08664	0.00045
15	72	72.08689	72.08692	72.08664	0.00025
20	98	98.08684	98.08688	98.08664	0.00020
26	128	128.08681	128.08685	128.08664	0.00017
33	162	162.08679	162.08683	162.08664	0.00015
102	512	512.08674	512.08678	512.08664	0.00010

TABLE II. Same as Table I, except that $\kappa=\mathcal{L}=\pi$, which corresponds to a short-range repulsive interaction. For each given state n , the error $\Delta_n^{\text{qm}}=E_n-E_n^{\text{qm}}=0.000\,09$. For comparison, if $\sigma=0.05$, then $E_{20}^{\text{sc}}=98.017\,64$; the error $\Delta_{20}^{\text{sc}}=0.001\,49$ is larger, but the semiclassical energy shift is unchanged to $O(10^{-3})$.

n	$E_n^{(0)}$	E_n	E_n^{qm}	E_n^{sc}	Δ_n^{sc}
7	32	32.02094	32.02104	32.01798	0.00296
15	72	72.01940	72.01949	72.01794	0.00146
20	98	98.01913	98.01922	98.01794	0.00119
26	128	128.01899	128.01908	128.01794	0.00105
33	162	162.01891	162.01901	162.01794	0.00097
102	512	512.01879	512.01888	512.01792	0.00087

estimates of their shifts under perturbation accurate to $O(10^{-3})$ in the case of long-range repulsive interactions, and to $O(10^{-2})$ in the case of short-range repulsive interactions. The numerical results for attractive interactions are an order of magnitude better in each case. Thus, the leading-order semiclassical approximation is more accurate for long-range interactions. This is to be expected since corrections to the Thomas-Fermi term are much more significant for short-range interactions. Numerically, we expect errors of at least $O(10^{-5})$ due to the approximate evaluation of the convolution integral [Eq. (28)] that gives the GCTF and of at least the same order from neglected corrections to the leading-order TF term. We also expect the semiclassical trace formulas to give accurate energy shifts for large quantum numbers. This is expected for two reasons: the first is that the GCTF is more accurate at large energies, and the second is that corrections to the Thomas-Fermi term are typically less important at large energies when interactions are repulsive. It is typical for the semiclassical approximation to become more accurate at larger energies and clearly this characteristic is found in the data when interactions are repulsive.

For long-range interactions, the perturbation is quite slowly varying on the scale of \mathcal{L} (the length of the well). Generally speaking, from quantum mechanics, we know that a flat perturbation causes all unperturbed levels to shift by the same amount. Thus, the quantum energy shifts are expected to be much the same for all levels when the rate of change of the interaction potential is small. For short-range interactions, there is more variation in the amount by which the low-lying singlets are shifted, but for higher energies the quantum shifts again become similar. The same characteristics are evident in the semiclassical data; the (leading-order)

semiclassical trace formulas yield the same shift for all singlets when the interaction is long-range, whereas there is some variation in the shifts when the interaction is short-range.

Note that both quantum and semiclassical perturbation theory are more accurate for long-range interactions. Furthermore, when the interaction is repulsive, $\Delta_{\text{qm}}^{\text{SR}}/\Delta_{\text{qm}}^{\text{LR}} \approx 3$, whereas $\Delta_{\text{sc}}^{\text{SR}}/\Delta_{\text{sc}}^{\text{LR}} \approx 6$ for all singlets (except the $n=102$ singlet), where the superscripts LR and SR denote long-range and short-range, respectively. The error in the smooth average density of states should account for the factor of 2. Finally, a close inspection of the quantum data to $O(10^{-8})$ reveals that the error from quantum perturbation theory slowly declines as the quantum number is increased when the interaction is short-range, but steadily increases when the interaction is long-range. (This is true regardless of whether the interaction is attractive or repulsive.) There is no such distinction for the leading-order semiclassical approximation; it simply improves at higher energies when the interaction is repulsive or becomes worse at higher energies when the interaction is attractive.

The results for attractive interactions are counterintuitive. The semiclassical energy shifts are more accurate (and often by an order of magnitude) for attractive interactions as compared to repulsive interactions. (It is worthwhile to mention here that a similar finding has been reported elsewhere [21].) There is no obvious reason to expect that the formalism of Sec. II should be more accurate for attractive interactions ($\epsilon < 0$) than for repulsive interactions ($\epsilon > 0$). There is another anomaly for attractive interactions; for moderate to large energies ($E \geq 100$), the semiclassical error increases. This is unexpected since the GCTF is, in general, more ac-

TABLE III. Same as Table I, except that $\epsilon=-0.1$, which corresponds to a long-range attractive interaction. The error $\Delta_n^{\text{qm}}=E_n-E_n^{\text{qm}}=0.000\,03$ for each given state n .

n	$E_n^{(0)}$	E_n	E_n^{qm}	E_n^{sc}	Δ_n^{sc}
7	32	31.91284	31.91287	31.91313	0.00029
15	72	71.91305	71.91308	71.91313	0.00008
20	98	97.91309	97.91312	97.91312	0.00003
26	128	127.91312	127.91315	127.91312	$O(10^{-6})$
33	162	161.91314	161.91317	161.91313	0.00001
102	512	511.91319	511.91322	511.91312	0.00007

TABLE IV. Same as Table II, except that $\epsilon = -0.1$, which corresponds to a short-range attractive interaction. For $n=26, 33, 102$, the error $\Delta_n^{\text{qm}} = E_n - E_n^{\text{qm}} = 0.00009$, whereas for $n=7, 15, 20$, the error $\Delta_n^{\text{qm}} = 0.0001$.

n	$E_n^{(0)}$	E_n	E_n^{qm}	E_n^{sc}	Δ_n^{sc}
7	32	31.97887	31.97896	31.98075	0.00188
15	72	71.98041	71.98051	71.98071	0.00030
20	98	97.98068	97.98078	97.98071	0.00003
26	128	127.98082	127.98092	127.98070	0.00012
33	162	161.98090	161.98099	161.98070	0.00020
102	512	511.98103	511.98112	511.98069	0.00034

curate at large energies. One possible explanation is that corrections to the Thomas-Fermi term can be significant at large energies if the interaction is attractive [19].

In short, apart from some interesting trends that require further study, good estimates of the perturbed singlet energies can be obtained from simply identifying the center of the appropriate spectral lines to a specified accuracy. We expect the symmetry-broken trace formulas to produce inaccurate results for large interaction strengths. One instance where this expectation turns out to be false occurs when the interaction is long-range (e.g., $\kappa = 1/\mathcal{L} = 1/\pi$). In this case, we find that the subset of spectral lines of the quantum CGDOS that are poorly reproduced by the GCTF in the medium-range ($\kappa = 1$) or short-range ($\kappa = \mathcal{L} = \pi$) cases is actually rather accurately reproduced by the GCTF for moderately large interaction strengths. In such a case, we can proceed as before to obtain estimates of the perturbed singlet energies. It is particularly interesting to consider individual singlets and track the error as the interaction strength is increased. A representative example is given in Table V. It is a pleasant surprise that the semiclassical error is less than 1% when $\epsilon = 1$. Even when the spectral line produced by the GCTF differs appreciably from the quantum spectral line (see, for example, the perturbed $E_{15}^{(0)} = 72$ singlet in the bottom right window of Fig. 1), we can still (although it is perhaps less meaningful) extract a semiclassical energy by identifying the maximum of the non-Gaussian line to a specified accuracy. Exemplary results obtained for the $E_{20}^{(0)} = 98$ singlet are given in Table VI, and although the way in which these energies are obtained is less unequivocal than before, the results are nevertheless accurate.

We return now to the multiplet states. After the interaction is turned on, the energy levels that were degenerate (when $\epsilon = 0$) split apart and shift by differing amounts relative to the unperturbed multiplet energy. For $\epsilon \ll 1$, the spacing between perturbed levels is very small, in fact, most of them are still essentially degenerate. Even when $\epsilon = 1$, the quantum splittings are still typically quite small if the interaction is long-range (e.g., $\kappa = 1/\pi$) or medium-range (e.g., $\kappa = 1$). In such cases, the GCTF still adequately reproduces the quantum CGDOS (see Fig. 4). It should be kept in mind that individual Gaussian lines will not be resolved when σ is larger than the spacing between energy levels. If the spacing between several levels is much smaller than σ , then a superposition of all the corresponding Gaussian lines will appear as only one Gaussian-like line, and the amplitude of that line indicates the number of levels embodied.

It is not clear from these computations whether the perturbed trace formulas can actually reproduce a genuine splitting. To answer this question, we could simply use very small variances, but this is computationally intensive, and as we have already discussed, the GCTF becomes less accurate if orbits with very large actions are included in the sums. The other approach is to drastically increase the interaction strength so that the spacings between perturbed levels become wider. Except at large energies, we expect the semiclassical analysis to break down completely for $\epsilon \gg 1$, but we can evaluate the GCTF for a nonweak interaction strength, for instance $\epsilon = 5$, and still expect reasonably accurate results. The splitting of some typical multiplets under a nonweak interaction is shown in Fig. 5. Clearly, first-order semiclassical perturbation theory cannot reproduce the quantum splittings. In fact, it appears that all spectral lines generated by

 TABLE V. The evolution of the $n=102$ singlet state of the symmetric irrep under perturbation by a long-range ($\kappa = 1/\pi$) repulsive interaction. The first column specifies the interaction strength, and the second column the exact quantum energy shift (i.e., $\delta E = E_{102} - E_{102}^{(0)}$). The third and fourth columns give the corresponding energy shifts obtained from quantum and semiclassical perturbation theory, respectively, and the fifth and sixth columns give the absolute error of these energy shifts relative to the exact quantum energy shift. Notice that (for the middle three entries) $\Delta_{\text{sc}} \approx 2.75\Delta_{\text{qm}}$.

ϵ	δE	δE_{qm}	δE_{sc}	Δ_{qm}	Δ_{sc}
1/10	0.0867	0.0868	0.0866	$O(10^{-5})$	0.0001
1/3	0.2889	0.2893	0.2878	0.0004	0.0011
1/2	0.4330	0.4339	0.4306	0.0009	0.0024
2/3	0.5770	0.5785	0.5728	0.0015	0.0042
1	0.8643	0.8678	0.8560	0.0035	0.0083

TABLE VI. The evolution of the $n=20$ singlet state of the symmetric irrep under perturbation by a short-range ($\kappa=\pi$) attractive interaction. The columns are as described in the caption of Table V except that the state in question is different (i.e., $\delta E=E_{20}-E_{20}^{(0)}$, etc.). Notice that (for the middle three entries) $\Delta_{sc} \approx 2\Delta_{qm}$. For comparison, when $\kappa=1$ and $\epsilon=-1$, then $\delta E=-0.5208$, $\delta E_{sc}=-0.5166$, and $\Delta_{sc}=0.0042$.

ϵ	δE	δE_{qm}	δE_{sc}	Δ_{qm}	Δ_{sc}
-1/10	-0.0193	-0.0192	-0.0193	0.0001	$O(10^{-5})$
-1/3	-0.0652	-0.0641	-0.0629	0.0011	0.0023
-1/2	-0.0986	-0.0961	-0.0932	0.0025	0.0054
-2/3	-0.1326	-0.1281	-0.1242	0.0045	0.0084
-1	-0.2024	-0.1922	-0.1889	0.0102	0.0135

the GCTF are shifted by the same amount (relative to the unperturbed energy) regardless of whether they correspond to singlet or multiplet states. So it is clear that when the spacing between perturbed levels is $O(\sigma)$ or larger, the leading-order perturbed trace formulas will not accurately reproduce the quantum CGDOS, however it is pleasing to observe that when the splittings are small compared to σ , the GCTF continues to work quite well even for a nonweak interaction strength such as $\epsilon=5$. Of course, the inability of (first-order) semiclassical perturbation theory to reproduce quantum splittings is a fundamental deficiency only when the particles are identical. However, the issue of computational expense remains even if the particles are nonidentical. Although there are no exact degeneracies (when $\epsilon=0$) in that case, there are still many near degeneracies, a characteristic of the fact that the unperturbed system is integrable.

IV. CONCLUSION

Any weak interparticle interaction can be thought of as a symmetry-breaking perturbation, and it is then possible to apply the results of the perturbative theory developed by Creagh [12] to obtain the trace formulas for a weakly interacting two-body system. Two weakly interacting identical point particles in a square well serves as the simplest nontrivial example to which the theory can be applied. The analysis of this problem adequately illustrates many general aspects of a calculation in higher dimensions. In fact, precisely the same analysis would apply to dynamical orbits that derive from isolated one-particle “libration” orbits in higher-dimensional billiards (regardless of the stability of these orbits). Two examples would be the primitive orbits along the minor and major axes of the two-dimensional elliptic billiard, and the isolated “diameter orbit” of the two-dimensional stadium billiard. It is important to understand that while we could have applied the ideas of Refs. [9,11] to analyze the example we studied in this paper, we cannot apply these ideas to the two examples we have just mentioned above. In such cases, we can only use the ideas of Creagh. The generality of Creagh’s perturbative theory makes it ultimately most useful for the analysis of weak interactions.

The correspondence between semiclassical and quantum perturbation theory in the context of the few-body problem can be summarized as follows: Quantum perturbation theory

predicts shifts in energy after an interaction is turned on, and in semiclassical perturbation theory, these shifts are due to the action shifts of the periodic orbits. The quantum theory uses only unperturbed quantum information (i.e., the unperturbed eigenstates), and the semiclassical theory uses only unperturbed classical information (i.e., the unperturbed periodic orbits).

For the square-well example, the perturbed contributions of all the nonprimitive heterogeneous and dynamical orbits were calculated, and it was possible to obtain a closed form for all of the action shifts. The fact that the perturbed contributions could be computed for all nonprimitive orbits is quite significant because we could then pursue a full quantization. Actually, Creagh’s perturbative theory is not meant to be used for the purpose of full quantization, but we have shown that the coarse-grained quantum density of states can be reproduced from summing the perturbed contributions of each periodic orbit family. Good numerical estimates of the quan-

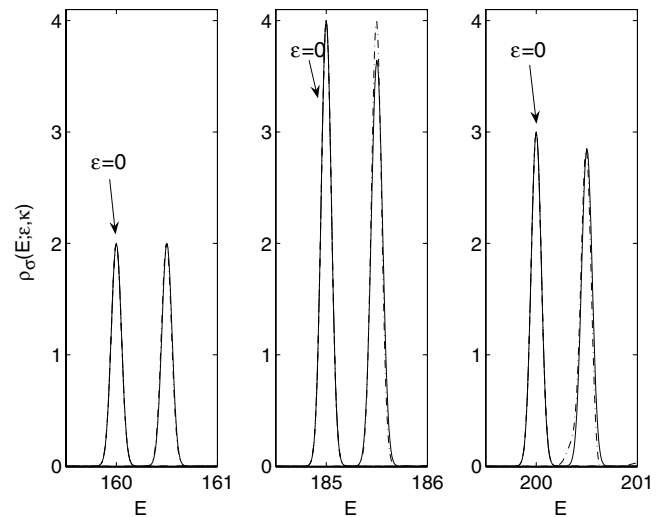


FIG. 4. The coarse-grained density of states (CGDOS) in the presence of a moderate strength ($\epsilon=1$) and medium-range ($\kappa=1$) interparticle interaction. Three different energy windows are shown typifying the effect of a moderate perturbation on different multiplets (doublet, quartet, and triplet). The solid line is the exact quantum CGDOS [Eq. (27)], and the dashed-dotted line is the semiclassical CGDOS obtained from the Gaussian-convolved trace formula (26). The amplitude cutoff $\delta=10^{-6}$, and the variance $\sigma=0.05$. The unperturbed multiplet lines ($\epsilon=0$) are included for reference.

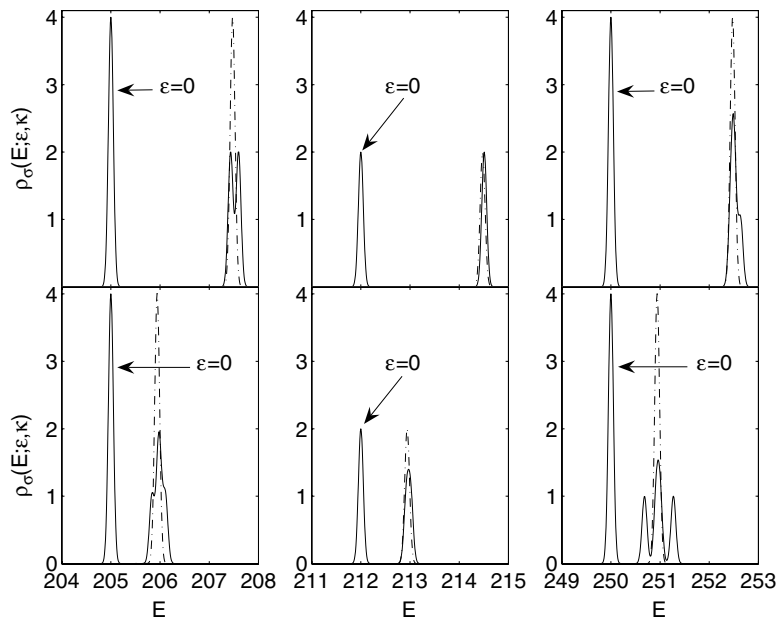


FIG. 5. The coarse-grained density of states (CGDOS) in the presence of a nonweak ($\epsilon=5$) interparticle interaction. As in Fig. 4, different energy windows are shown. In the upper three windows, the interaction is medium-range ($\kappa=1$), and in the lower three windows, the interaction is short-range ($\kappa=\pi$). The solid line is the exact quantum CGDOS [Eq. (27)], and the dashed-dotted line is the semiclassical CGDOS obtained from the Gaussian-convolved trace formula (26). The amplitude cutoff $\delta=10^{-6}$, and the variance $\sigma=0.05$. The unperturbed multiplet lines ($\epsilon=0$) are included for reference.

tum singlet energies can be obtained (even for moderate interaction strengths) by summing the Gaussian-convolved perturbed trace formulas and identifying the center of Gaussian spectral lines (or the maximum of non-Gaussian spectral lines) to a specified accuracy. This is significant because the system, although simple, is still nonintegrable. At present, the periodic orbit quantization of nonintegrable systems is not viable. The analysis of the square-well example suggests that it might be viable to achieve semiclassical quantization in other few-body problems that consist of weakly interacting particles in a one-dimensional potential, such as a system of two or three weakly interacting particles in a one-dimensional quartic oscillator. The semiclassical analysis of this example would actually be a good future project.

Some general conclusions (based on the results in Tables I–IV) can be made regarding the accuracy of the leading-order semiclassical approximation: (i) it is more accurate for long-range interactions since corrections to the Thomas-Fermi term are more important for short-range interactions; (ii) it is more accurate for attractive interactions, at low energies; (iii) for repulsive interactions, the semiclassical estimates monotonically improve as the energy increases, whereas for attractive interactions, the semiclassical estimates are best for the low-lying states, but then become less accurate for higher quantum numbers. The last property is surprising since the GCTF itself is more accurate at higher energies. It is possible that corrections to the Thomas-Fermi term are more significant at higher energies for attractive interactions (see, for example, Ref. [19]). More work is required to understand why (in the case of attractive interactions) the semiclassical approximation is best for small quantum numbers and why it slowly becomes worse for higher quantum numbers. To pursue these questions, we would have to go beyond the leading-order semiclassical approximation, that is, we would have to compute corrections to the Thomas-Fermi smooth term and possibly go so far as to evaluate the convolution integrals that produce the GCTF exactly (i.e., numerically). Exact numerics would provide a

more precise comparison between quantum and semiclassical perturbation theory.

The perturbed trace formulas fail to reproduce the multiplet splittings observed from quantum mechanics. Each (degenerate) spectral line of a multiplet was found to shift by the same amount after the interaction was turned on. This of course is a fundamental problem only when the particles are identical. It would be interesting to see whether genuine splittings would appear if the analysis of the time-translation symmetry breaking was carried out to higher order in perturbation theory.

Another extension is to explicitly include the particle exchange symmetry and decompose the total density of states (studied here) into the separate densities of symmetric and antisymmetric states. To take on this problem, it would be a matter of understanding how the dynamical pseudoperiodic orbits [7] are affected by interactions. For the square-well example, these orbits are isolated, and so the type of analysis discussed in Ref. [9] for the treatment of isolated orbits under perturbation would apply.

A complete analysis of the example studied in this paper would also involve a thorough investigation of the Gutzwiller limit ($\epsilon \gg 1$), and an estimation of the range of interaction strengths for which the Gutzwiller theory and the perturbative theory yield similar results. This is an essential first step in developing a uniform theory that could describe the entire range of behaviors between the noninteracting and strongly interacting limits. A genuine “uniform approximation” should recover the Gutzwiller theory in the limit where the interaction is arbitrarily strong and therefore reproduce the results of a direct application of the Gutzwiller trace formula. The semiclassical framework introduced here for the weak-coupling limit should be regarded as a first step toward this more ambitious goal.

A major research initiative is to apply the theory to higher-dimensional systems. An immediate and important example is two weakly interacting particles in a two-dimensional square billiard. This is the higher-dimensional

version of the problem we studied here. Of course, the increase in dimensionality introduces some complications. The one-particle periodic orbits of the two-dimensional square are more intricate (although still piecewise linear), but more importantly, the one-particle orbits themselves occur in continuous families. The treatment of the dynamical orbits in this paper assumes that the one-particle dynamics is free of any continuous symmetry. In general, if there are other continuous symmetries, then these must be properly accounted for in the analysis. The theory of Ref. [12] can still be applied, but of course the analysis would be more involved than the analysis of problems like the one we studied here [22]. The treatment of the heterogeneous orbits would also

require revision and would further require knowledge of higher-order \hbar corrections. The effect of interactions would have to be worked out for each of these higher-order corrections. An important reason for choosing the square-well example here is that \hbar corrections are not required for the analysis. We hope to study higher-dimensional systems in more detail in a future paper.

ACKNOWLEDGMENTS

We thank Rajat Bhaduri for useful discussions. This work was financially supported by the Natural Sciences and Engineering Research Council of Canada (NSERC).

-
- [1] M. Brack and R. K. Bhaduri, *Semiclassical Physics* (Addison-Wesley, Reading, MA, 1997).
- [2] M. C. Gutzwiller, *J. Math. Phys.* **8**, 1979 (1967); **10**, 1004 (1969); **11**, 1791 (1970); **12**, 343 (1971).
- [3] M. C. Gutzwiller, *Chaos in Classical and Quantum Mechanics* (Springer-Verlag, New York, 1990).
- [4] H.-J. Stöckmann, *Quantum Chaos: An Introduction* (Cambridge University Press, Cambridge, 1999).
- [5] P. Cvitanović *et al.*, *Classical and Quantum Chaos: A Cyclist Treatise* (Niels Bohr Institute, Copenhagen, 2000), and references therein.
- [6] J. Sakhr and N. D. Whelan, *Phys. Rev. A* **62**, 042109 (2000).
- [7] J. Sakhr and N. D. Whelan, *Phys. Rev. E* **67**, 066213 (2003).
- [8] M. V. Berry and M. Tabor, *Proc. R. Soc. London, Ser. A* **349**, 101 (1976); *J. Phys. A* **10**, 371 (1977).
- [9] A. M. Ozorio de Almeida, in *Quantum Chaos and Statistical Nuclear Physics*, edited by T. H. Seligman and H. Nishioka, Lecture Notes in Physics Vol. 263 (Springer, Berlin, 1986); A. M. Ozorio de Almeida, *Hamiltonian Systems: Chaos and Quantization* (Cambridge University Press, Cambridge, 1988).
- [10] A. M. Ozorio de Almeida and J. H. Hannay, *J. Phys. A* **20**, 5873 (1987).
- [11] S. Tomsovic, M. Grinberg, and D. Ullmo, *Phys. Rev. Lett.* **75**, 4346 (1995); D. Ullmo, M. Grinberg, and S. Tomsovic, *Phys. Rev. E* **54**, 136 (1996).
- [12] S. C. Creagh, *Ann. Phys. (N.Y.)* **248**, 1 (1996).
- [13] M. Brack, S. C. Creagh, and J. Law, *Phys. Rev. A* **57**, 788 (1998).
- [14] M. Brack, P. Meier, and K. Tanaka, *J. Phys. A* **32**, 331 (1999).
- [15] M. Brack, M. Öggen, Y. Yu, and S. M. Reimann, *J. Phys. A* **38**, 9941 (2005).
- [16] J. K. Cullum and R. A. Willoughby, *Lanczos Algorithms for Large Symmetric Eigenvalue Computations* (Birkhäuser, Boston, 1985).
- [17] G. H. Golub and C. F. van Loan, *Matrix Computations* (Johns Hopkins University Press, Baltimore, 1989).
- [18] H. M. Sommermann and H. A. Weidenmüller, *Europhys. Lett.* **23**, 79 (1993).
- [19] B. K. Jennings, R. K. Bhaduri, and M. Brack, *Phys. Rev. Lett.* **34**, 228 (1975).
- [20] The linewidth could be interpreted as a measure of the uncertainty in the semiclassical energy. If so, then a peak maximum that occurs at E_{sc} gives a semiclassical energy $E_{sc} \pm \sqrt{2}\sigma$. However, to compare with the exact quantum-mechanical energies, we are then forced to use small values for σ (for example, 10^{-6}), which (as explained later) actually increases the numerical error associated with the GCTF. A semiclassical energy shall be identified with the position of a peak maximum and no further interpretation of the peak width will be assigned.
- [21] The average density of states for a system of interacting fermions in one dimension was briefly considered in Ref. [18], where it was found that the semiclassical approximation is quite accurate for attractive interactions, but largely overestimates the cumulative density of states when there are repulsive interactions.
- [22] We should point out that additional symmetries are complications not only in higher-dimensional systems; the same issue would come up for two identical particles in a one-dimensional harmonic oscillator.